Journal of Cultural Heritage 81 (2026) 142–154

Contents lists available at ScienceDirect

Journal of Cultural Heritage

journal homepage: www.elsevier.com/locate/culher

VSI: TECHNART 2025

Lab-based XANES spectroscopy for chemical and structural characterization of pigments in cultural heritage science

Gianluca Santagati[a,b], Michela Botticelli[a,b,*], Tecla Arcidiacono[a,b], Claudia Caliri[a,b], Francesca Falcone[a,b], Costanza Miliani[a], Jens Rauschenberger[d], Eva Luna Ravan[a,c], Francesco Paolo Romano[a,b]

[a] Istituto di Scienze del Patrimonio Culturale, Consiglio Nazionale delle Ricerche (CNR-ISPC), Italy
[b] Istituto Nazionale di Fisica Nucleare, Laboratori Nazionali del Sud (INFN-LNS), Italy
[c] Department of Science of Antiquities, University of Rome 'Sapienza', Italy
[d] HP Spectroscopy GmbH, Forggenseestr. 25, 68219, Mannheim, Germany

ARTICLE INFO

Article history:
Received 31 December 2025
Accepted 7 July 2026

Keywords:
XANES
Laboratory-based XAS
Cultural heritage materials
Pigment characterization
Oxidation state analysis
Linear combination fitting (LCF)

ABSTRACT

This study presents a laboratory-based XANES protocol optimized for the chemical characterization of historical pigments in cultural heritage materials. Using a refined lab-scale X-ray absorption spectroscopy set-up, we demonstrate the capability to extract chemically meaningful near-edge features - such as oxidation-state–dependent edge shifts, pre-edge features, and spectral shoulders - that enable reliable discrimination among pure pigment systems. The protocol was benchmarked against synchrotron XANES reference data and supported by ab-initio simulations, confirming the preservation of diagnostically relevant near-edge information under laboratory energy resolution constraints. Linear Combination Fitting (LCF) was employed to obtain semi-quantitative insights into pigment mixtures. The protocol was first tested on well-defined binary mixtures simulating the co-existence of original pigments and their potential deterioration products and was subsequently applied to unknown and compositionally complex mixtures, where the identification of different materials is critical for the study of ancient and modern artists' materials. Laboratory XANES applied to optimized thin sections was demonstrated to reproducibly capture As(III) spectral features in orpiment-based mock-ups, and clearly distinguish it from As_2O_3, demonstrating its potential for chemical speciation studies in micrometric paint layers. While laboratory-based XANES does not replace synchrotron measurements in terms of ultimate spectral resolution, it enables reproducible discrimination of oxidation states and local coordination environment and supports semi-quantitative phase assessment in contexts where synchrotron access is not feasible. Overall, the results establish a robust methodological framework for extending XANES-informed chemical interpretation into routine heritage science workflows, proving that laboratory XANES, compared to synchrotron experiments, can be less invasive and preserve sufficient near-edge sensitivity for reliable speciation and semi-quantitative bulk analysis, despite the lower spectral resolution.

1. Introduction and research aim

Understanding the composition and structural organization of pigment materials in cultural heritage artifacts is essential for their knowledge, conservation, and historical interpretation. Pigments not only provide visual and aesthetic significance but also serve as markers for provenance, dating, and material degradation processes. Analytical methods that offer precise chemical information are therefore vital for conservation and restoration practices [1].

Among the wide array of analytical and imaging techniques employed in this context, spectroscopic methods such as X-ray fluorescence (XRF) and X-ray diffraction (XRD), Raman spectroscopy, and Fourier-transform infrared spectroscopy (FTIR) are commonly used due to their portability and non-invasiveness, which makes them highly compatible with the uniqueness of an artwork and its accessibility [2,3]. However, each method has specific applicability: XRF provides elemental information without insight into oxidation states while XRD can only probe into crystalline compounds; Raman and FTIR are sensitive to surface inorganic/organic compo-

* Corresponding author at: Istituto di Scienze del Patrimonio Culturale, Consiglio Nazionale delle Ricerche (CNR-ISPC), Italy.
E-mail address: michela.botticelli@cnr.it (M. Botticelli).

https://doi.org/10.1016/j.culher.2026.07.007

nents but may suffer from fluorescence interference and limited penetration depth. These techniques can be complemented by X-ray Absorption Spectroscopy (XAS), providing information on the local chemical and structural environment within complex pigment matrices [4–8]. XAS may overcome the limitations other analytical techniques have. Unlike diffraction-based techniques, XAS does not require long-range structural order, making it particularly suitable even for the investigation of amorphous or poorly-crystalline pigments and their alteration products, that are known to evolve as highly-superficial thin (micrometer or even sub-micrometer range) surface layers while the bulk material remains unchanged. Furthermore, recent advances in laboratory-based XAS systems (henceforth lab-XAS) now allow high-quality spectra to be obtained without the need for synchrotron radiation, thus overcoming major logistical barriers and enabling routine, in-house analysis.

Either in its XANES (X-ray Absorption Near Edge Structure) or EXAFS (Extended X-ray Absorption Fine Structure) modalities, XAS offers peculiar capabilities for probing the local chemical environment of specific elements in the complex and heterogeneous systems that often characterize cultural heritage objects [7,9,10], and particularly artists' paints, where a metal chromophore is usually involved. XANES delivers element-specific insights into oxidation states, electronic structure, and coordination geometry, and allows for semi-quantitative analysis through spectral deconvolution and linear combination fitting (LCF) [11,12]. In the last two decades these features have been proven especially valuable in the study of historical pigments [11,13–17] and the degradation pathways affecting ancient [18–23] or modern artists' pigments [12,24–29], one of the earliest and most exploited field of application of XAS for cultural heritage [30,31]. In addition, considerable effort has been devoted to investigating the influence of binding media on pigment stability and long-term conservation using XAS-based approaches [32,33].

EXAFS, on the other hand, extends the analysis beyond the absorption edge to provide structural information such as interatomic distances, the type and number of neighbouring atoms, and local geometric configurations [7]. This level of structural detail is critical for identifying specific molecular phases, distinguishing between polymorphs, and understanding the bonding environment around absorbing atoms. While EXAFS data is not included in the present study, its integration into future work is anticipated. It will complement the chemical information obtained from XANES and further enhance the interpretive framework for complex pigment materials.

Regardless of the explored energy range, the hard X-ray region (5–35 keV) being most commonly employed in the earliest experimentations and recently giving way to the tender (1.5–5 keV) and soft (50–1500 eV) regimes [34,35], the exploitation of XAS at synchrotron beamlines (henceforth SR-XAS) has continuously grown, evolving from large beams suited for bulk analysis to micro- or nano-focused beams. The process has been fostered by the development of highly-focused beamlines [17,36], which are of primary importance when studying: (1) pigment manufacturing/application processes, often in complex paint mixtures where different micrograins can exhibit distinctive chromophores; (2) deterioration processes, which are known to affect the surface at the micro-scale (usually tens of microns). In parallel, efforts have been made to reduce or eliminate the dependency on a sample prepared through demanding and time-consuming procedures. Depending on the experimental configuration, SR-XAS typically requires specific sample preparation and mounting, and measurements can be performed either in transmission or reflection geometries. Transmission is the most straightforward configuration, the sample being prepared as a homogeneous pellet or thin (tens of micrometers) paint cross-section. In this geometry, the incident beam passes through the sample and is partially absorbed before reaching the detector. This configuration also allows full-field (FF-XAS) measurements if the beam is unfocused and the detector is, for example, a complementary metal oxide semi-conductor (CMOS) camera [6,35]. Alternatively, measurements can be carried out in reflection geometry, in which the sample is positioned at an angle with respect to both the incident beam and the detector, allowing either single point analysis (fixed sample) or mapping (scanned sample). The absorption signal is then obtained using indirect detection modes, most commonly X-ray fluorescence yield (XFY) or total electron yield (TEY), often introducing self-absorption effects. Advantages and limitations of XFY versus TEY in pigment analysis have already been addressed [37], and provide a useful framework for evaluating their potential compared to laboratory-based implementations. In brief, XFY provides a more bulk-sensitive probe, making it particularly suitable for stratified or heterogeneous systems such as paint layers. In contrast, TEY is a surface-sensitive technique, characterized by a shallow probing depth and generally lower susceptibility to radiation damage due to the reduced interaction volume. However, TEY measurements are strongly influenced by surface conditions and require relatively homogeneous, sufficiently large, and uncoated samples, as the presence of varnishes or surface contaminants can significantly affect the signal. The XRF mode also allows full-spectral (FS) μ-XANES imaging, recording stacks of several μ-XRF maps around the edge of the element of interest with variable energy step size before/at/after the pre-edge peak and absorption edge. FS-XAS has the advantage of being more representative than single-point μ-XANES coupled to single-energy μ-XRF mapping, as it produces a datacube of XANES spectra per pixels with lower fluence measurements. However, there are some intrinsic limitations compared to μ-XANES, such as longer acquisition times and lower spectral resolution [38].

Despite its analytical strength, the routine application of XAS in heritage science is still limited by its dependence on synchrotron radiation facilities, which are not only geographically restricted but also subject to high competition for beamtime and complex scheduling logistics. These limitations have prevented the incorporation of XAS as a routine analytical tool in the workflow of heritage conservation laboratories [39].

As a response to these challenges, recent developments in lab-XAS instrumentation have opened new avenues for in situ and more flexible elemental and structural characterization of several materials [40,41], although the potential of this approach has not been explored on artwork and historical samples yet. Advances in source brightness, detection systems, and analytical software now permit meaningful data collection with benchtop systems, bridging the gap between the chemically relevant information content provided by SR-XAS and the practical constraints of routine laboratory operations. Concerns that have received increasing attention in SR-XAS studies for heritage science deal with radiation damage or radiation-induced side effects, respectively defined as any optically visible or non-apparent chemical or structural modification of a pigment induced by beam exposure [42]. It is well established that intense and bright micro-focused beams can impart localised changes to specific pigments, like Prussian blue [24,43,44], ultramarine [34,45], or chrome yellows [46]. By contrast, the implications of beam-induced effects under laboratory conditions have not yet been addressed in heritage science, to the best of the authors' knowledge.

In this work, we present a comprehensive experimental protocol for laboratory-based XANES (lab-XANES) measurements applied to historical pigments relevant to cultural heritage studies. The experiments were performed at the XRAYLab of CNR-ISPC in Catania using a Mo anode X-ray tube coupled with an optimized von Hamos Highly Annealed Pyrolytic Graphite (HAPG) crystal spectrometer and a 2D position- and energy-sensitive detector.

The protocol embraces technical setup, sample preparation strategy, data acquisition procedures, and spectral analysis workflows, including LCF for semi-quantitative assessment of selected pigment systems. Where available, the results are validated against SR-XAS measurements and compared with simulations, demonstrating the reliability and applicability of the lab-based approach for pigment characterization. The proposed scheme is robust, reproducible, and compatible with multi-analytical workflows. It enables the determination of oxidation states, observation of subtle edge-structure features linked to local coordination, and the semi-quantitative assessment of pigment mixtures such as goethite/hematite or the presence of any deterioration product in a pigment matrix (for instance CuO in copper-carbonate greens/blues). It also explores the potential of thin-section analysis to study micrometric surface alteration in paint fragments. In respect to these aspects, we show the results representative of the instrument potential.

The long-term objective is to establish a standardized lab-XAS protocol that can be reliably applied to the analysis of both ancient and modern pigments within small-scale facilities. The setup will actively contribute to the network of key fixed research facilities within the FIXLAB platform of E-RIHS - the European Research Infrastructure for Heritage Science (https://www.e-rihs.eu/e-rihs-catalogue-of-services/, last accessed 08/06/2026) by developing and maintaining advanced instrumentation for diagnostics and archaeometry. By integrating detailed guidelines for sample preparation, measurement conditions, and data processing, the protocol supports the routine application of XANES in heritage science and establishes the basis for future EXAFS integration toward full structural elucidation. Understanding the potential and limitations of lab-XAS enables a realistic assessment of which chemically relevant near-edge features can be reliably accessed within a compact laboratory footprint (4.0 m × 1.0 m), without aiming to replicate the ultimate energy resolution of synchrotron facilities. The design of an XAS experiment is of primary importance. Several aspects impact on the success of an experiment and need to be addressed before starting any scientific experiment: (1) the objectives; (2) the information that can realistically be obtained; and (3) the procedures that will be followed for a successful conclusion [47]. The present study aims to define the type and level of information that can realistically be obtained using a lab-XAS system when addressing specific objectives relevant to the study of pigment materials, and to establish an optimized protocol to achieve meaningful and reproducible results. Within this framework, the goal is not to replace SR-XAS, but to develop a robust and transferable methodology for extracting chemically interpretable information under laboratory conditions.

As sample preparation can strongly affect XAS data quality [48], particular attention was devoted to the optimization of pigment preparation procedures, including sample concentration, thickness, and homogeneity. When dealing with unique or highly valuable objects, as is often the case in heritage science, defining in advance the minimum amount of material required for a reliable XAS experiment is also a critical aspect of the methodological design.

Overall, this research provides a comprehensive framework for evaluating how a lab-XAS facility can address key questions in heritage science, ranging from the characterization of ancient materials to the study of conservation treatments and environmentally driven alteration phenomena in artworks.

2. Materials and methods

2.1. Sample materials and preparation

Pigment standards were selected to represent historically significant materials commonly used in the creation of artworks and in their subsequent restoration. The pigment selection presented here was intentionally designed as a first step to evaluate the potential of lab-XAS, focusing on compounds containing relatively light absorbing elements, which represent a challenging case for laboratory measurements. These included Fe-based (goethite, hematite), and Cu-based (malachite, azurite, CuO) pigments. Samples were prepared as pressed pellets using a hydraulic press.

Pellets were fabricated by first grinding and homogenising the powder materials to ensure correct particle size distribution, followed by mixing with a cellulose binder. Cellulose (microcrystalline powder, SA 435236) was selected for its chemical inertness, low X-ray absorption, and ability to improve mechanical compactness and homogeneity of the pellet, particularly when the concentration determined to have optimum absorption from the target element was too low [48]. Each pellet had a diameter of 13 mm, providing sufficient surface area for reliable beam interaction and suiting the sample holder diameter (15 mm). To ensure consistency across all samples, pellets were prepared using a standardized protocol, enhancing comparability between samples and reduced experimental variability. Specific aspects were optimized: grinding (agate ball mill dry grinding for 10 min in agate mortar), applied pressure (8 tons), pressing duration (2 min) and binder proportion. For the latter, the optimal mass and thickness of each pellet were calculated using the XASmassQt software [49], targeting an absorption edge jump ($\Delta\mu x$) close to 1 [48], to avoid the potential thickness effect due to inhomogeneity in the wafer [50]. This allowed a balance between total absorption and signal-to-noise ratio, critical for accurate XAS analysis. The edge jump was checked with a fast run (1 min), and concentrations were adjusted in case this was found to be below 1, especially for samples where the analyte was not the only component of a pigment mixture. Optimized pigment:binder ratios for each commercial pigment are reported in Table S1 and can serve as reference for sample preparation before any future lab-XAS measurement. The powder mixture was then pressed into compact pellets using a laboratory hydraulic press, setting the pressure to 8 tons for 2 min.[1]

The applicability of the method to paint fragments prepared as thin sections was also investigated, as this approach is particularly relevant for the study of degraded surface layers with micrometric thickness. Such sample preparation is especially advantageous in the presence of an oil binder, which hinders the direct preparation of homogeneous pellets from paint layers. Mock-up samples of orpiment in oil (75 wt% 10700 Kremer pigment and 25 wt% cold-pressed linseed oil) were prepared by grinding the pigment in an agate mortar prior to mixing. The resulting paint was applied, in duplicate, onto microscope glass slides using a controlled-thickness film applicator, yielding layers approximately 200 µm thick to ensure uniformity and reproducibility. Thin sections of 40 and 60 µm thickness were then obtained from the surface of each mock-up using a manual rotary microtome (Epredia HM325) in dry room-temperature conditions. During sectioning, the glass slide was secured with a clamp and a blade (MX35 Premier Plus, Low Profile, 50PK for hard tissues, 34° cutting angle, 0.24 mm thickness) was used to produce slices.

As 60 µm represents the maximum thickness achievable with the microtome under the adopted conditions, an additional measurement was performed on a folded 60 µm section, increasing the total thickness to 120 µm. This approach allowed evaluation and optimization of the resulting absorption step and assessment of the feasibility of this preparation method for lab-XAS measurements. We also verified that the lateral dimensions of the thin sections were compatible with the projected beam footprint on the

[1] These were determined to be the best pressure and time values for achieving a compact wafer. Note that they deviate from what recommended for routine XAS applications [48].

Table 1
projected beam size on the sample (5 cm distance to source) for the 2nd-order XANES measurements at the K edge of the elements of interest for the pigments discussed in this paper.

Elem.	*Energy (eV)*	*Meridional Ø (mm)*	*Sagittal Ø (mm)*
Mn	6539	1.3	2.3
Fe	7112	1.1	2.1
Co	7709	0.9	1.9
Cu	8979	0.7	1.7
As	11867	0.4	1.2

Fig. 1. Lab-XAS setup at XRAYLab, CNR ISPC (Catania, Italy); red inset: internal view illustrating the core components (X-ray source, sample holder, He-purged cells and HAPG von Hamos crystal in XANES configuration, and hybrid detector), aligned along two motorized optical rails; blue inset: a close-up of the sample holder with one position holding a small fragment of cinnabar paint.

sample (at a 5 cm source–sample distance) for XANES measurements at the arsenic K-edge, ensuring optimal interaction between the incident beam and the analysed area (Table 1):

Reference metal foils for energy calibration, pigment pellets or thin sections were mounted on an aluminium sample holder using Kapton tape, chosen for its low X-ray absorption and chemical stability. This mounting strategy guaranteed stable measurement conditions and optimal interaction between the sample and the X-ray beam.

2.2. Instrumentation and setup

All XANES measurements were performed at the XRAYLab of CNR-ISPC using the lab-based hiXAS system designed and implemented by TU Berlin [51] and commercialized by HP Spectroscopy GmBH. The instrument offers a complete benchtop solution for either EXAFS or XANES analysis, integrating a molybdenum-anode X-ray tube operating at 20 kV and 1.5 mA, a von Hamos HAPG crystal spectrometer, and a large-area hybrid detector (Fig. 1). A dedicated software suite enables automated control, calibration, and spectral processing, facilitating batch measurements with minimal user intervention.

The X-ray tube and spectrometer cover an energy range from 4.5 to 25 keV, including the K-edges of 3d transition metals and L-edges of heavier elements, making the system suitable for a broad range of materials. In XANES mode, the system delivers a photon flux of approximately 1×10^6 ph/s at 8 keV. The spectrometer's HAPG crystal geometry (bending radius of R = 300 mm) ensures high detection efficiency and good signal-to-noise ratio, with a spectral resolving power of up to $E/\Delta E = 4000$ across the energy range.

The Dectris Eiger2 R 500K detector provides high spatial resolution (75 µm × 75 µm pixel size) and an extended dynamic range ($>10^9$ ph/s/mm²), ensuring reliable photon counting even under high-flux conditions. Its dual-threshold energy discrimination allows for precise spectral filtering and enhances signal-to-noise performance. With a maximum frame rate of 40 Hz and zero dead time, the detector supports rapid data acquisition, making it particularly suitable for time-resolved and in situ measurements. Its extended sensor layer (77.3 mm × 38.6 mm) is particularly suited for EXAFS measurements, as it covers the whole EXAFS spectral range, especially at its lower end. Its operational energy range—extending up to approximately 18–23 keV—covers the K-edge of most 3d transition metals and L-edge of heavier elements. The hybrid detector setup allows spatially resolved detection, supporting the assessment of sample homogeneity, and is mounted on a dual-axis translation stage to enable accurate alignment and focusing. A partial helium-purged environment (cells with Kapton windows) is used to reduce X-ray absorption by air and improve performance at lower energies, particularly below 10 keV.

The main components of the hiXAS instrument are mounted on a modular optical table and enclosed with integrated interlock system for safe operation. The lower part of the enclosure hosts control units and storage space. The X-ray source assembly includes a basic sample mount, designed to work in transmission and possibly support customer-provided specialized holders. Two long motorized translation stages allow precise positioning of the crystal and detector. The spectrometer crystal is mounted on a movable stage for remote alignment, while the detector is mounted on a second motorized stage, enabling independent optimization of detection geometry.

2.3. Measurement parameters

Energy calibration was performed using metal foils as references, following standard procedures [48]. These reference samples were measured at the beginning and end of each acquisition batch to monitor and correct any energy drift. Spectra were acquired in continuous scan mode across the K-edge of each element, with step sizes of 0.2 eV near the edge and 2–5 eV in the pre- and post-edge regions. Typical acquisition times for the reference were 60 min, while a good total measurement time for standard pigments with variable concentration and matrix composition was estimated to be 350 min (blank t_0 = 50 min, sample t_s = 300 min), after a series of tests.[2] Beam stability, count rates and dead-time correction were constantly monitored using the hiXAS acquisition software, and real-time visualization was used to adjust integration time and confirm spectral quality during the scan. This ensured consistency and high fidelity across datasets, particularly for samples analysed over extended timeframes.

2.4. Data processing and analysis

Spectra were processed using the Demeter software package (Athena), as described by Ravel and co-authors [52,53]. E_0 calibration and edge-step normalization were applied following best practices, and no smoothing was performed. These were carefully checked before applying the LCF, as preliminary data processing has strong impact on the goodness of the fit. The LCF method was applied in the energy range $-15 < E_0 < +35$ eV to quantify mixtures. For the mixtures at known concentration the fit was built on the experimental spectra (flattened) collected on pure pellets

[2] Short, averaged measurements were compared to long single measurements. A good compromise to have reasonable time measurement and acceptable signal-to-noise ratio for pure pigment analysis was determined to be: single measurement with total time of 300 minutes.

of each compound, namely malachite, azurite, Cu_2O and CuO — acquired under identical conditions using the same lab-XAS system — in line with methodologies applied in similar studies [54]. The energy range pre-edge features were analysed to support oxidation state attribution. Energy shifts observed across batches were corrected based on reference sample calibration. The LCF was eventually tested on unknown pigment mixtures, i.e. several commercial ochres where we expected to find a mixture of iron oxides and hydroxides, this time using synchrotron reference data. The comparison between lab-XANES spectra and synchrotron reference data was performed using spectra retrieved from established databases, providing well-characterized benchmarks for the investigated compounds. While the use of reference data acquired on independently prepared samples may introduce variability related to differences in sample preparation (e.g., pellet composition, density, and homogeneity), this comparison is intended primarily as a semi-quantitative validation of the laboratory setup, focusing on energy alignment and the overall spectral envelope rather than on a strict quantitative match. In addition, the use of such reference datasets is often necessary when samples with the exact target composition are not readily available or cannot be reproducibly prepared under controlled conditions. In this context, assessing the robustness of the LCF on partially unknown or complex mixtures is particularly relevant for pigments such as ochres, where the principal chromophore is generally known but additional iron-bearing phases may be present and not fully characterized, despite contributing to the XANES signal at the absorption edge.

2.5. Spectral simulation in FDMNES

XANES simulations were performed using the FDMNES code, which provides multiple-scattering (MST) and finite-difference (FDM) formalisms for the calculation of near-edge absorption spectra [55]. Unless otherwise stated, all simulations were carried out using the MST approach (Green keyword) together with muffin-tin potentials and the standard convolution procedure (Convolution). The crystallographic structures used as input (CIF files – see Table S2) were selected from crystallographic databases and correspond to room-temperature phases. For the copper-based compounds (CuO, Cu_2O and malachite), a spherical cluster radius of 5 Å was adopted, which was sufficient to ensure convergence of all spectral features. In these systems, no additional treatment of the core hole (SCFexc/screening) nor extra instrumental broadening beyond the default Lorentzian lifetime was required. For iron compounds, convergence tests indicated the need for larger clusters due to their extended electronic interactions and magnetic ordering. A decreasing-radius strategy was applied: starting from 8 Å up to 30 eV above the edge, then 7 Å up to 70 eV, 6 Å up to 100 eV, and finally 5 Å for the higher-energy region. This approach ensures accurate reproduction of the near-edge structure while reducing computational costs at higher energies. In α-Fe and α-Fe_2O_3 (hematite), the magnetic ground state was explicitly included using the Magnetism keyword, whereas FeO(OH) (goethite) was treated in its non-magnetic approximation.

3. Results and discussion

3.1. Spectral features, oxidation states, and local electronic environment

Before evaluating unknown samples, we validated the reliability and resolution of the lab-XAS setup through direct comparison with synchrotron data and FDMNES simulations, using both metal foils and pure compounds.

Fig. 2 illustrates the normalized Fe foil (3 µm thickness) spectrum acquired with our lab-based system in 1 h, a synchrotron reference from the XASLIB database (https://xaslib.xrayabsorption.org/spectrum/110/, last accessed 08/06/2026), and FDMNES simulation. The close agreement in edge shape and relative edge position indicates that the laboratory configuration preserves the diagnostically relevant near-edge features required for chemical interpretation, and confirms the internal consistency of the energy calibration. Similarly, Fig. 3 presents the XANES spectrum of a CuO pellet acquired with the lab-based system, in comparison with synchrotron data and theoretical modelling. The reproduction of near-edge features further supports the system's capability to characterize oxidized species, resolving edge features of the oxidized copper phase with high accuracy and consistency with synchrotron data, although it is less sensitive to EXAFS oscillations.

Fig. 3 also illustrates how theoretical modelling is more sensitive to pre-edge features and the first peak around the main edge, as already determined comparing experimental and simulated Cu-based standards [56].

To assess the system sensitivity to different oxidation states, we analysed a set of Cu standards —metallic copper, Cu_2O, and CuO. Each oxidation state displays distinct edge positions and white line intensities. As illustrated in Fig. 4, which compares the normalized spectra acquired with the lab-based XAS system, we could observe the shift of the absorption edge to higher energy with higher oxidation state [40].

The edge shift and spectral features confirm oxidation-state and sensitivity to characteristic features. Analysis of pre-edge and near-edge features also provides insights into the coordination geometry and ligand environment of the absorbing atoms.

In excellent agreement with previous studies [54], the characteristic low-energy near-edge feature associated with Cu(I) species was consistently observed at lower energies (at 8984 eV) with respect to the typical shoulder of Cu(II) compounds (below 8987 eV) within the internally calibrated dataset. The comparison between simulated and experimental K-edge energy values (Table 2) shows that the latter are within the uncertainty of the experimental energy calibration, demonstrating that oxidation-state–dependent spectral shifts can be reproducibly resolved under laboratory conditions.

The possibility to detect characteristic features in the XANES spectra, such as pre-edge peaks and shoulders, contributes to the identification of chemical differences, aiding in the detection of degradation products, such as CuO arising from malachite, for example after exposure to alkalis or heat [57].

Table 2
Simulated and experimental K-edge energies for Cu-based standards after the measurements shown in Fig. 4.

Compound	*Simulated E_k (eV)*	*Experimental E_k (eV)*
Cu	8979	8979
Cu_2O	8982	8982
CuO	8984	8984

3.2. Quantitative mixture analysis

To evaluate the capability of the lab-XANES system to discriminate and semi-quantitatively assess component contributions in pigment mixtures, we first analysed a set of synthetic samples of known composition. The application of an effective LCF to model degraded systems can provide a robust framework not only to identify but also to quantitatively assess the extent of transformation processes, thereby offering a useful tool to elucidate and monitor deterioration mechanisms in historical pigments. Hence, we explored the potential of the LCF method in the evaluation of several Cu-based systems like $Cu_2CO_3(OH)_2$/CuO (ratio 3:1), the oxide being a possible degradation product of basic copper carbonates, especially under high-temperature or oxidizing condi-

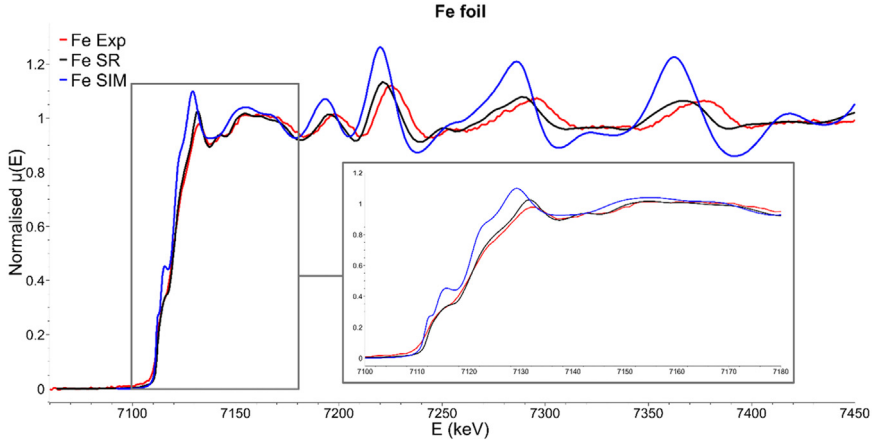

Fig. 2. Comparison between Fe metal foil XANES spectra: 1-hour laboratory measurement on a 3-μm-thick foil (red), synchrotron reference (black, https://xaslib.xrayabsorption.org/spectrum/110/, last accessed 08/06/2026), and FDMNES simulation (blue).

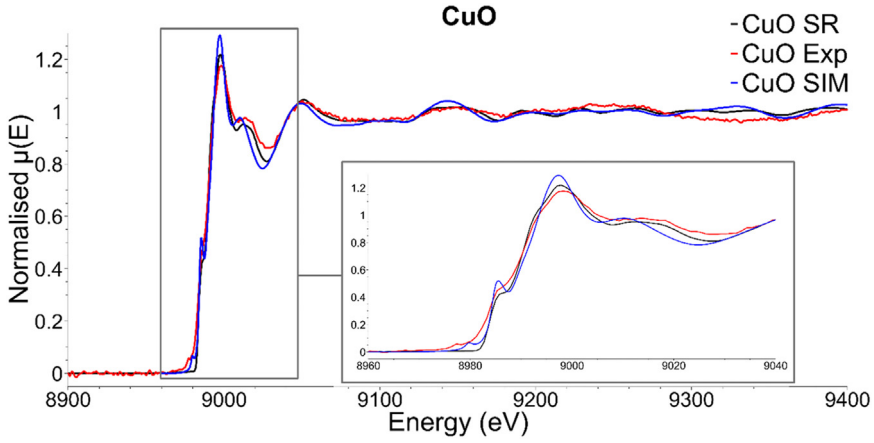

Fig. 3. Comparison between normalized CuO XANES spectra: 1-hour laboratory measurement (red) of a CuO pellet (see Table S1 for analyte:binder), synchrotron reference (black, data from https://xaslib.xrayabsorption.org/spectrum/87/, last accessed 08/06/2026), and FDMNES simulation (blue).

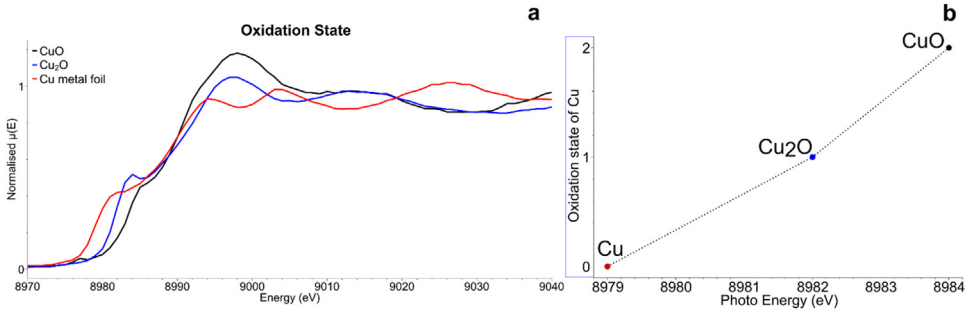

Fig. 4. Comparison between experimental normalized XANES spectra of different Cu compounds - Cu foil (red), Cu_2O (blue), and CuO (black) - acquired with the lab-based XAS system with acquisition time of 1 h (for sample preparation see Table S1) showing the E_0 shift with increase of the oxidation state (a) and the almost linear correlation between oxidation state and edge position (b).

tions [57]. Clear spectral differences between the copper carbonate, $Cu_2CO_3(OH)_2$, and the oxide CuO, were observed in the XANES spectra of the pure pellets, confirming the system's sensitivity to oxidation state and ligand field variations, as already reported in Gaur et al. [54], which assisted the goodness of the LCF. Applied to the known binary mixtures, the LCF demonstrated that the lab-XANES system could quantify pigment proportions within an estimated error of ±5%. These results are consistent with the reported accuracy thresholds in recent operando lab-XAS studies [58]. For instance, both carbonate/oxide mixtures yielded fitted values in close agreement with the known mass ratios (Table 3), the fitted curve showing very minor deviations from the experimental data (R factor = 0.0025661; chi-square = 0.01874) that may reflect matrix effects or particle size disparities [48].

Table 3
Summary of LCF results on known mixtures: comparison between nominal and fitted pigment ratios.

Mixture Type	*Known Ratio (%)*	*Fitted Ratio (%)*	*Error (%)*
Malachite/CuO	75 / 25	73 / 27	± 2
Azurite/CuO	75 / 25	76 / 24	± 1
Cu_2O/CuO	75 / 25	80 / 20	± 5

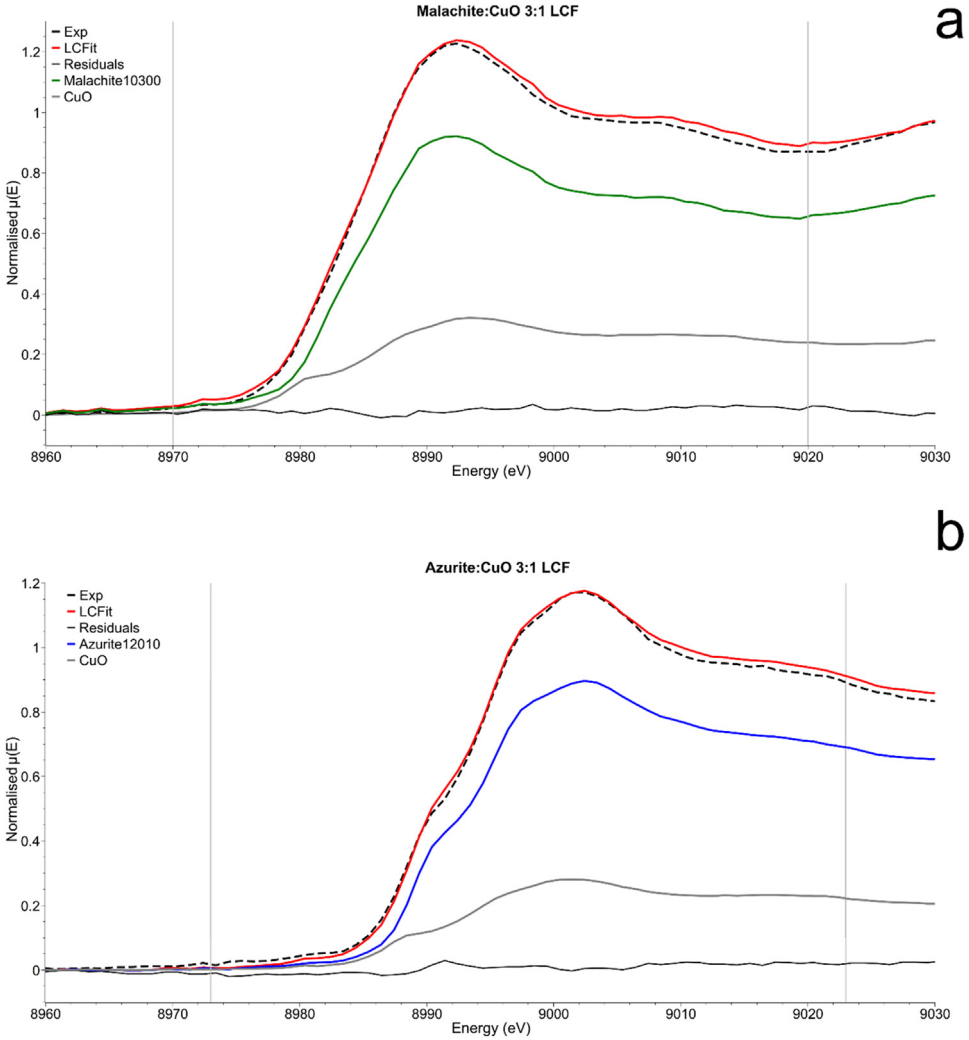

Fig. 5. Normalized XANES experimental spectrum of carbonate:oxide (3:1) mixtures (black dashed, a = malachite, b = azurite), LCF curve (red), with weighted reference carbonate (green/blue solid, respectively) and oxide (grey) spectra and the residual plot (black solid); pellet samples prepared as in Table S1.

Fig. 5a displays the analysis of the malachite/CuO mixture. The spectral differences between Cu(II) in malachite and CuO are sufficient to enable oxidation-state differentiation and component quantification. The LCF accurately determined the actual composition used to prepare the pellet, confirming that, under controlled conditions, lab-XANES can assess relative component contributions with good internal consistency.

Analogously, the percentages estimated by the LCF method for the azurite:CuO mixture (Fig. 5b) was 76% and 24% respectively, with an error of ± 1%, and the values obtained for the statistical goodness-of-fit parameters are: R-factor = 0.001401 and chi-square = 0.01249.

The mixture Cu_2O:CuO gave the highest error (5%), the estimated mass ratio being 80 to 20% (R factor = 0.0006486; chi-square = 0.00576). Observed spectral differences (Fig. 6), especially in the CuO pre-edge region, which impact the LCF estimation, can be attributed to a combination of factors, including variability in sample preparation (e.g., homogeneity and packing), as well as intrinsic variations in signal-to-noise ratio across laboratory measurements. In addition, slight differences in data processing (e.g., normalization and background subtraction procedures) may contribute to subtle variations in the intensity and shape of pre-edge features.

Following the validation on a system of known composition, we applied the same analytical protocol to several commercial

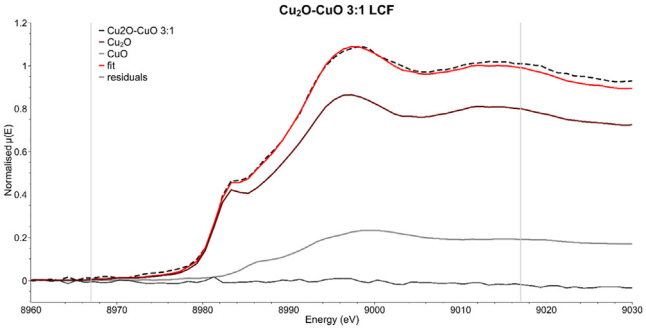

Fig. 6. Normalized XANES experimental spectrum of Cu_2O:CuO (3:1) mixture (black dashed), LCF curve (bright red), together with weighted reference Cu_2O (dark red), and CuO (grey) spectra and residual plot (black solid); pellet samples prepared as in Table S1.

ochres with unknown proportions of iron-bearing phases. Overall, the XANES spectra acquired for Fe-based pigments exhibited well-resolved spectral features consistent with known reference compounds. The distinction between goethite and hematite is evident through differences in pre-edge intensity and edge position, in agreement with recent DFT-based investigations [59]. Particularly, the red sample, which we expect to be hematite-predominant, ex-

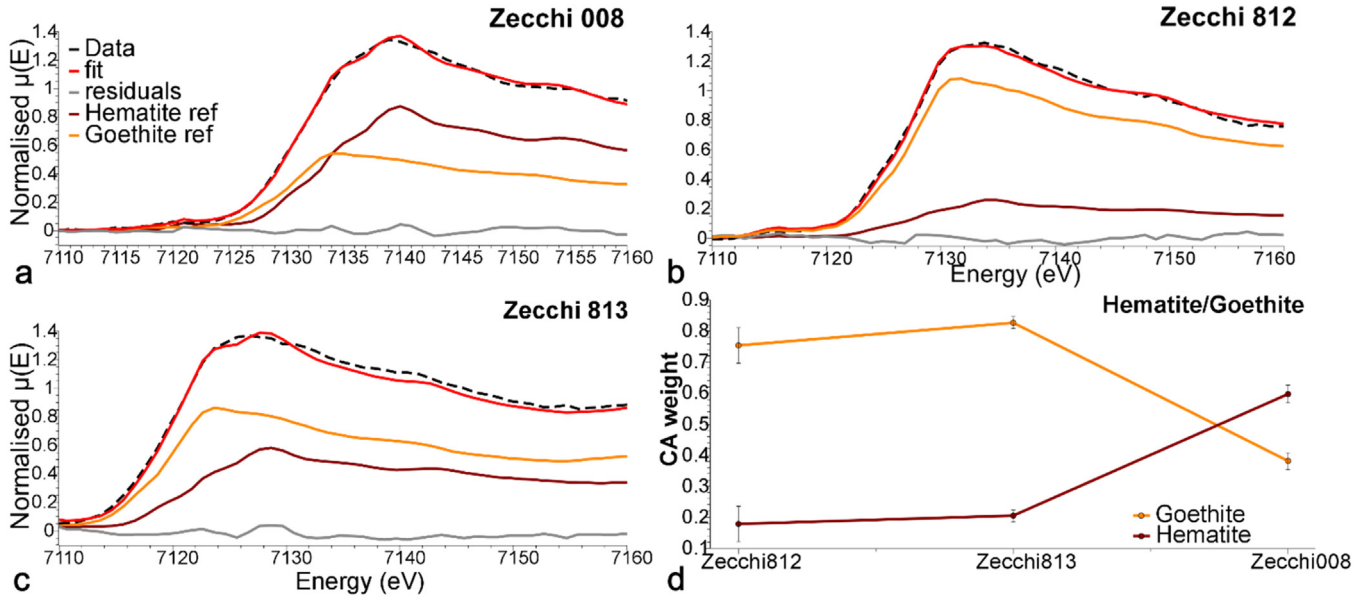

Fig. 7. Normalized lab-XANES experimental spectra (black dashed) of different commercial ochres (a = Red ochre Sinopia, b = Pale yellow ochre, c = Natural Sienna earth) prepared as in Table S1, with LCF curve (red solid) to determine hematite (brown solid, https://xaslib.xrayabsorption.org/spectrum/104/, last accessed 08/06/2026) and goethite (yellow solid, data from https://xaslib.xrayabsorption.org/spectrum/116, last accessed 08/06/2026) content; d illustrates how the predominant colouring agent (CA) varies in weight from sample to sample, hematite having the highest content in the red sinopia and goethite in the Pale yellow ochre.

Table 4
Summary of LCF results on unknown mixtures: determination of hematite and goethite content in different commercial ochres, with statistics from the fit (R factor and χ^2) and E_0 fit with error.

	R factor	X^2	Goethite ref				Hematite ref			
			weight	error	E_0	error	weight	error	E_0	error
Zecchi008	0.001811	0.01592	0.38	0.03	4.4	0.2	0.60	0.03	7.7	0.1
Zecchi812	0.003071	0.02823	0.75	0.06	1.3	0.1	0.18	0.06	2.2	0.6
Zecchi813	0.006419	0.06203	0.60	0.06	−6.3	0.2	0.40	0.06	−3.7	0.4

hibited the spectral features typically observed for Fe_2O_3, with a pre-edge, a shoulder, an intense white line and a post-edge shoulder (Fig. 7a). However, their positions shifted towards higher energies compared to reference XANES spectra [60]. For this, in the LCF procedure we refined the edge position.

Ochres are commonly composed of clay, quartz, and iron oxides, where the relative proportions of goethite and hematite influence the hue [61]. The developed lab-based protocol allows for non-destructive quantification of the main mineral phases imparting the hue to the pigment, relevant for the classification and conservation of historical pigments. Iron in ochres could also come from minor phases like lepidocrocite, ankerite or natrojarosite [62–64]. Consequently, the goodness of the LCF resulted improved when we did not force weights to sum to 1. In this case, the LCF coefficients should be interpreted as spectral weights reflecting the dominant iron-bearing phase contributing to the XANES signal, rather than as absolute phase fractions, due to the possible presence of additional minor components and matrix effects not explicitly included in the fitting model. The LCF performed on each sample determined the predominant colouring agent using hematite and goethite reference spectra. On the red ochre sinopia (Fig. 7a), it yielded a composition of approximately 60% hematite and 38% goethite. The Natural Sienna earth exhibits intermediate spectral features (Fig. 7c) with peak positions and intensities indicative of 60% goethite and 40% hematite. Finally, in the pale-yellow ochre goethite predominates (Fig. 7b), its content being 75% with 18% hematite.

A summary of the LCF results comparing the content of the colouring agent (CA in Fig. 7d) – either hematite or goethite – in the different ochres analysed by the lab-XANES system is given in Table 4.

These values are consistent with compositional ranges reported in literature for natural ochres [64,65]. As expected, hematite predominates in the red sample, while goethite displays the highest content in the pale-yellow sample, 60% being enough for hematite to impart the intense red hue to the Sinopia (Zecchi 008), consistently with previous findings on archaeological samples [66].

3.3. Thin section analysis

The use of thin sections enables the study of superficial layers of a paint sample, which is of primary importance for the definition of any chemical change occurring when a deterioration process is ongoing. Controlled variation of sample thickness is essential during the preparation steps, as it provides a simplified representation of the uppermost layers in a paint fragment, allowing to probe averaged chemical information across micrometric layers. In order to assess the feasibility of XANES measurements under laboratory conditions, we measured thin sections prepared with different thickness to determine the maximum absorption step achievable with this type of preparation for orpiment in oil mock-ups.

Lab-XANES spectra acquired from both pellet and thin sections exhibit the characteristic features of As(III) species, with excellent consistency in the position of the white line observed between 11869 and 11870 eV (compare maxima in the first-derivative plot of Fig. 8a inset), in agreement with reference data [67,68]. As expected, the absorption edge step varies with sample preparation, with the optimum value $\Delta\mu x \approx 1$ achieved for the pellet prepared according to the calculated pigment:cellulose ratio (15:85 mg). For thin sections, the 40 μm thickness was insufficient to yield an adequate absorption edge step, whereas the best compromise was ob-

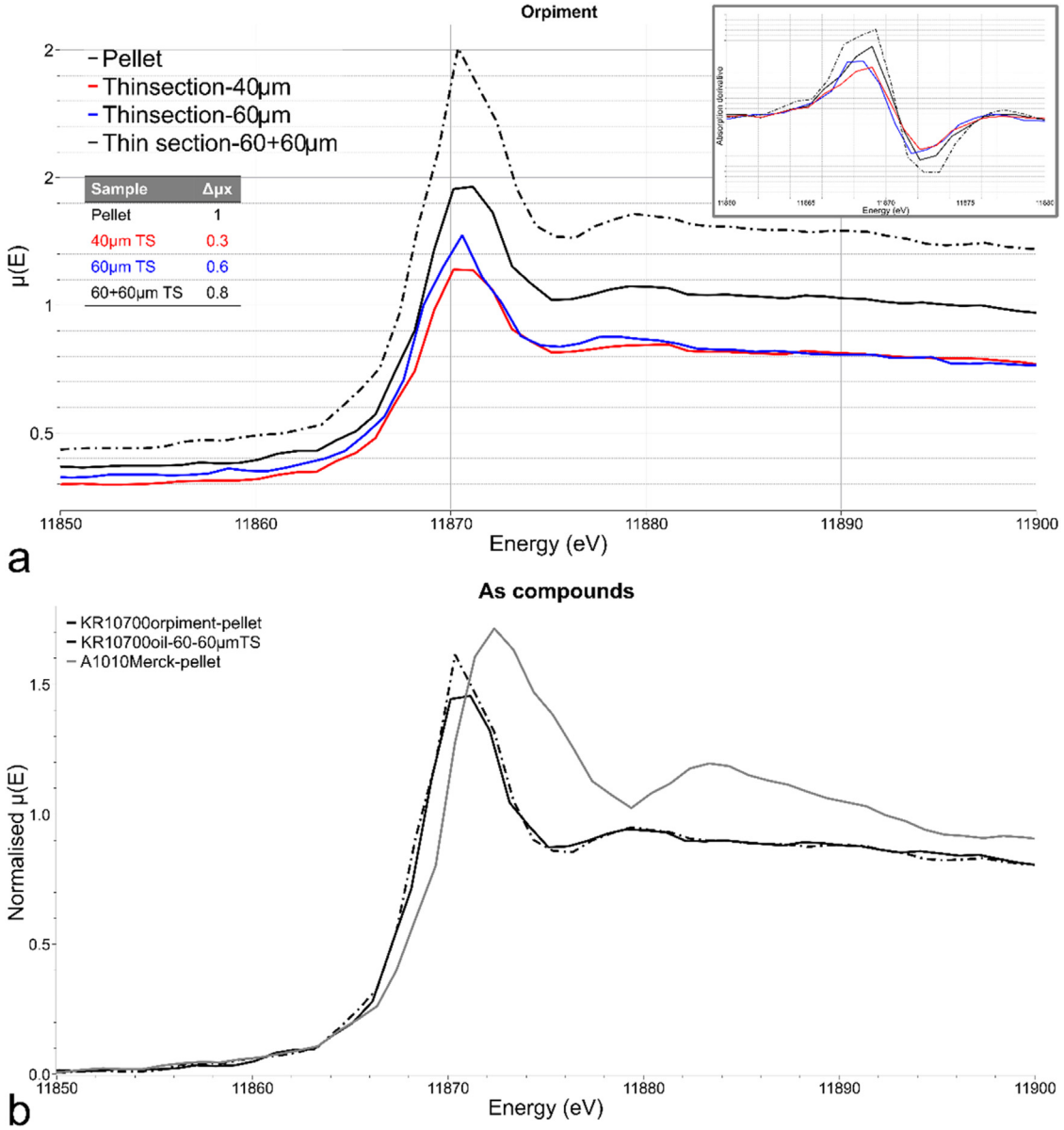

Fig. 8. a) lab-XANES experimental spectra of orpiment: pure in a cellulose pellet (dotted black line), and with oil binder as thin section of different thicknesses (red line = 40 µm, blue = 60 µm, solid black = sandwiched 60+60 µm); b) comparison of orpiment pellet (dotted black) and sandwiched thin section (solid black) with a possible alteration product, As_2O_3 (A1010 Merck chemical, pellet, grey plot).

tained with the sandwiched 60µm-thick paint fragment, resulting in $\Delta\mu x \approx 0.8$ (solid black line in Fig. 8a).

Comparison with a reference As_2O_3 pellet (Fig. 8b), a common deterioration product of arsenic-based pigments [69], demonstrates that its spectral features can be clearly identified and distinguished from those of orpiment. In particular, As_2O_3 exhibits a white line at slightly higher energy (11872 eV) and a characteristic post-edge feature at approximately 11883 eV, both of which are resolved in the lab-XANES data, fostering the distinction from orpiment, irrespective of whether the latter is prepared as a pellet or a "sandwiched" thin section.

3.4. Methodological considerations and limitations

The experimental protocol proved robust and repeatable across multiple sample types, despite the inherent limitations of the laboratory source compared to synchrotron radiation [51,58]. Within the optimised acquisition time, signal quality was sufficient for meaningful interpretation of both qualitative and quantitative data. Although acquisition times are substantially longer in laboratory measurements (hours) compared to synchrotron experiments (seconds/minutes), several factors point to a much lower probability of any radiation-induced side effect or damage to occur during lab-XAS measurements: (1) the use of a low-power source, typically operating at 20 kV and 1 mA (20 W), as in mobile or handheld instrumentation [70,71]; (2) the significantly lower photon flux achievable with the lab-based instrument - order of 10^6 versus the typical values (10^8–10^{12} ph/s) of a synchrotron experiment [17,30,44,46]; a much larger beam size - millimetric rather than micrometric, as in the most recent SR configurations used to study pigment deterioration [17,22,23,46,72,73].

Overall, the optimisation protocol here described for a selected set of pigments incorporates a series of radiation-damage mitigation factors consistent with those addressed by Bertrand et al. [42,74]. As noted above, some of these are intrinsic, as they arise from instrumental design. Additional mitigation is achieved

through experimental validation: having estimated sample quantity and acquisition time —sufficient to achieve adequate absorption step and data quality as described in Section 2.1 —avoids repeated measurements and the probability of radiation damage, and hence prevents data misinterpretation, especially in speciation analysis of faded artworks [38].

While SR-XAS remains the method of choice for high spatial resolution studies requiring micrometric beam sizes and detailed stratigraphic mapping, the lab-XAS system presented here offers complementary capabilities that are particularly relevant for cultural heritage research. It reduces the need for extensive preparation of standards or mock-up samples typically required to optimise experimental conditions and mitigate radiation damage when using high-brilliance, micro-focused sources [74]. This makes the approach particularly suitable for preliminary or systematic investigations of radiation-sensitive pigments, like As-based yellows and reds, where minimising damage is critical.

Although spatial resolution is limited compared to synchrotron micro-beams, information from paint fragments can still be accessed through the analysis of prepared thin sections with controlled thickness, as demonstrated in this work. The optimisation of a thin-sectioning protocol and its use for pigment analysis provides a simplified representation of the most superficial paint layers, allowing to probe averaged chemical information across micrometric layers. Lab-XANES retains sensitivity to oxidation state and local coordination environment, making it applicable to the study of amorphous or poorly crystalline materials (e.g., glasses and certain ceramics), where long-range order is not required. However, matrix effects and sample heterogeneity remain potential challenges, particularly for elements at low concentration.

In parallel, the LCF method proved particularly sensitive to the data processing protocol, which must be as consistent as possible across different pigments mixtures. A continuous optimisation of sample preparation protocol, acquisition parameters and data processing steps, as preliminarily done in the present study, is a key aspect to minimise sampling, improve spectral reproducibility and, consequently, the robustness and reliability of the LCF analysis, while mitigating radiation damage. Future integration with structural methods like XRD will allow the integration of quantitative results. Further characterization of the EXAFS mode will support structural resolution at the atomic scale, as proposed in prior synchrotron-driven heritage studies [75].

4. Conclusions and future perspectives

This study demonstrates the feasibility and analytical relevance of a lab-XANES protocol for the characterization of pigments used in cultural heritage. By employing a compact laboratory XAS setup based on a Mo anode X-ray source coupled with a wavelength-dispersive von Hamos HAPG crystal spectrometer, it is possible to extract chemically meaningful near-edge features that enable the identification of oxidation states, the discrimination of local coordination environments, and the comparative assessment of pigment systems sharing the same absorbing element. Because both laboratory and synchrotron XAS require sampling, the first approach generally implying higher amounts (in the order of tens of milligrams), and given the uniqueness and value of cultural heritage materials, in this work particular attention was devoted to optimising the sampling and preparation protocol for a comprehensive list of paint materials. This provides practical guidance for heritage science professionals on how to minimize the amount of material required for lab-XAS while ensuring sufficient absorption step and adequate data quality, starting from compounds having light absorbing elements. It also proposes a detailed workflow to optimize the procedure and reduce user-dependent variability, both for pellets and thin sections. Investigations on additional pigments, including those based on heavier elements such as chromium and lead, are currently ongoing and will further extend the applicability and validation of the proposed methodology.

The results show that, although lab-XANES does not achieve the ultimate energy resolution attainable at synchrotron facilities, it preserves a significant fraction of the diagnostically relevant near-edge information required for chemical interpretation. In controlled systems, such as well-defined binary mixtures, the LCF provides constrained semi-quantitative estimation of relative component contributions, while in more complex materials it supports the identification of dominant phases when interpreted within a carefully defined fitting framework. Demonstrating the effectiveness of LCF applied to well-defined binary mixtures, this study preliminarily highlights the capability of lab-XANES to distinguish between pigments and their alteration products. Extending this approach to artificially aged mock-ups and pellets prepared with varying pigment–alteration product ratios will enable a more accurate determination of detection limits and the assessment of the system's sensitivity to early-stage degradation processes. In this sense, an important step would be the combination of lab-XANES with other quantitative methods like XRD with Rietveld refinement.

These capabilities are particularly relevant in heritage science contexts, especially when access to synchrotron facilities is limited but laboratory-based investigations on sampled materials are necessary to address routinely targeted chemical and mineralogical questions. In this framework, lab-XAS represents a valuable complementary approach to SR-XAS, enabling systematic and reproducible studies under controlled laboratory conditions within small-scale research facilities. SR-XAS provides higher flux, resolution, and flexibility in detection modes (transmission, XFY, and TEY), but it involves stricter experimental constraints and greater risk of radiation damage. The described lab-based system configures as a more accessible, less invasive alternative for routine heritage science. The proposed protocol benefits from low photon flux and optimized conditions, eluding self-absorption issues typical of the XRF mode. However, radiation effects from prolonged exposure still require systematic evaluation. Future work could assess beam-induced changes in pigment samples introducing interim data monitoring and extending the study to a wider range of materials. This would potentially benefit from a multimodal approach combining lab-XAS with complementary techniques to correlate spectroscopic and structural information to any morphological, compositional or structural changes induced by beam exposure.

The results achieved on thin sections demonstrate that analysis by lab-XANES on this type of sample may represent a viable and effective approach for systematic, low-impact investigation of pigment degradation. Despite the intrinsic limitations in flux and spatial resolution compared to synchrotron techniques, the method enables reliable identification of chemical speciation within micrometric superficial layers, from where deterioration typically starts and progresses. Further research could extend this approach to thin sections derived from a broad range of pigment/pigment mixture mock-ups, before and after artificial ageing, to systematically evaluate the effects of degradation under controlled conditions.

Future developments will also focus on extending the present protocol to EXAFS analysis, enabling access to interatomic distances and coordination numbers that will further strengthen the structural interpretation of complex pigment systems and their deterioration pathways. In parallel, continued optimization of sample preparation strategies and ongoing improvements in spectrometer performance, detector efficiency, and data modelling are expected to enhance spectral fidelity, robustness, and analytical throughput,

consolidating lab-XAS as a reliable and versatile tool for heritage science research within fixed laboratory infrastructures.

Web references

- https://catalogue.e-rihs.eu/service/93/x-ray-absorption-fine-structure-spectroscopy-xafs, last accessed 08/06/2026.
- https://xaslib.xrayabsorption.org/spectrum/110/, last accessed 08/06/2026.
- https://xaslib.xrayabsorption.org/spectrum/87/, last accessed 08/06/2026.
- https://xaslib.xrayabsorption.org/spectrum/116/, last accessed 08/06/2026.
- https://xaslib.xrayabsorption.org/spectrum/104/, last accessed 08/06/202.

Funding

This research was funded by the projects: H2IOSC “Humanities and Cultural Heritage Italian Open Science Cloud” [IR0000029, 616 CUP B63C22000730005, NRP M4C2, Investment 3.1, Funded by the European Union – NextGenerationEU]; CHANGES, SPOKE 5 “Science and Technologies for Sustainable Diagnostics of Cultural Heritage” [PE 0000020, CUP B53C22003890006, NRP M4C2 Investment 1.3, Funded by the European Union – NextGenerationEU]; SAMOTHRACE, “Sicilian MicronanoTech Research And Innovation Center” [ECS 622 00000022, CUP B63C22000620005, NRP M4C2 Investment 1.5, Funded by the European Union – NextGenerationEU]; The support by E-RIHS.it, Italian national node of the Eu (MUR FOE ERIHS IT and PON Ricerca e Innovazione 2014-2020, CCI: 2014IT16M2OP005) is also acknowledged.

Author contributions

All authors have read and agreed to the published version of the manuscript.

Data availability

The main data is contained within the article and supplementary material. Additional data presented in this study is available on request from the corresponding author.

Supplementary materials

Supplementary material associated with this article can be found, in the online version, at doi:10.1016/j.culher.2026.07.007.

References

[1] D’Amico S., Venuti V.. Handbook of cultural heritage analysis. vol. 1–2. 2022. https://doi.org/10.1007/978-3-030-60016-7.
[2] R. Mazzeo (Ed.), Analytical Chemistry for Cultural Heritage, Springer International Publishing, Cham, 2017, doi:10.1007/978-3-319-52804-5.
[3] M.P. Colombini, I. Degano, A. Nevin, Analytical Chemistry for the Study of Paintings and the Detection of Forgeries, Springer, Cham, 2022, doi:10.1007/978-3-030-86865-9.
[4] M. Cotte, J. Susini, J. Dik, K. Janssens, Synchrotron-based X-ray absorption spectroscopy for Art Conservation: looking back and looking forward, Acc. Chem. Res. 43 (2010) 705–714, doi:10.1021/ar900199m.
[5] M. Cotte, J. Szlachetko, S. Lahlil, M. Salomé, V.A. Solé, I. Biron, et al., Coupling a wavelength dispersive spectrometer with a synchrotron-based X-ray microscope: a winning combination for micro-X-ray fluorescence and micro-XANES analyses of complex artistic materials, J. Anal. At. Spectrom. 26 (2011) 1051, doi:10.1039/c0ja00217h.
[6] M. Cotte, E. Pouyet, M. Salomé, C. Rivard, W. De Nolf, H. Castillo-Michel, et al., The ID21 X-ray and infrared microscopy beamline at the ESRF: status and recent applications to artistic materials, J. Anal. At. Spectrom. 32 (2017) 477–493, doi:10.1039/c6ja00356g.
[7] Janssens K., Cotte M. The use of XAS and Related Methods in Cultural Heritage Investigations. International Tables for Crystallography Volume I: X-ray absorption Spectroscopy and Related Techniques, vol. I, 2023, p. 1039–46. https://doi.org/10.1107/S1574870720004802.
[8] F. Vanmeert, S. De Meyer, A. Gestels, E.A. Clerici, N. Deleu, S. Legrand, et al., in: M.P. Colombini, I. Degano, A. Nevin (Eds.), Non-invasive and Non-Destructive Examination of artists’ pigments, Paints and Paintings by Means of X-ray Imaging Methods, Analytical chemistry for the study of paintings and the detection of forgeries, 2022, pp. 317–357, doi:10.1007/978-3-030-86865-9_11.
[9] D. Creagh, Chapter 1 synchrotron radiation and its use in art, archaeometry, and cultural heritage studies, in: D. Creagh, D. Bradley (Eds.), Physical Techniques in the Study of art, Rchaeology and Cultural Heritage, Elsevier, 2007, pp. 1–95, doi:10.1016/S1871-1731(07)80003-0.
[10] L. Bertrand, Chapter 2 synchrotron imaging for archaeology, art history, conservation, and palaeontology, in: D. Creagh, D. Bradley (Eds.), Physical Techniques in the Study of art, Archaeology and Cultural Heritage, Elsevier, 2007, pp. 97–114, doi:10.1016/S1871-1731(07)80004-2.
[11] F. Bardelli, G. Barone, V. Crupi, F. Longo, G. Maisano, D. Majolino, et al., Iron speciation in ancient Attic pottery pigments: a non-destructive SR-XAS investigation, J. Synchrotron. Radiat. 19 (2012) 782–788, doi:10.1107/S0909049512023990.
[12] L. Monico, G. Van der Snickt, K. Janssens, W. De Nolf, C. Miliani, J. Dik, et al., Degradation process of lead chromate in paintings by Vincent van Gogh studied by means of synchrotron X-ray spectromicroscopy and related methods. 2. Original paint layer samples, Anal. Chem. 83 (2011) 1224–1231, doi:10.1021/ac1025122.
[13] E. Chalmin, F. Farges, C. Vignaud, J. Susini, M. Menu, G.E. Brown, Discovery of unusual minerals in Paleolithic black pigments from Lascaux (France) and Ekain (Spain), AIP Conf. Proc. 882 (2007) 220–222 volAIP, doi:10.1063/1.2644480.
[14] I. Reiche, S. Röhrs, J. Salomon, B. Kanngießer, Y. Höhn, W. Malzer, et al., Development of a nondestructive method for underglaze painted tiles—Demonstrated by the analysis of Persian objects from the nineteenth century, Anal. Bioanal. Chem. 393 (2009) 1025–1041, doi:10.1007/s00216-008-2497-7.
[15] M.O. Figueiredo, T.P. Silva, J.P. Veiga, A XANES study of cobalt speciation state in blue-and-white glazes from 16th to 17th century Chinese porcelains, J. Electron. Spectros. Relat. Phenom. 185 (2012) 97–102, doi:10.1016/j.elspec.2012.02.007.
[16] K. Janssens, M. Alfeld, G. Van der Snickt, W. De Nolf, F. Vanmeert, M. Radepont, et al., The use of synchrotron radiation for the characterization of artists’ pigments and paintings, Annu. Rev. Anal. Chem. 6 (2013) 399–425, doi:10.1146/annurev-anchem-062012-092702.
[17] L. Monico, K. Janssens, M. Cotte, S.M. Webb, F. Vanmeert, V. Gonzalez, et al., Advanced X-ray techniques to study the alteration of pigments in paintings, Riv. Nuovo Cimento 48 (2025) 315–434, doi:10.1007/s40766-025-00070-7.
[18] M. Cotte, J. Susini, N. Metrich, A. Moscato, C. Gratziu, A. Bertagnini, et al., Blackening of Pompeian cinnabar paintings: x-ray microspectroscopy analysis, Anal. Chem. 78 (2006) 7484–7492, doi:10.1021/ac0612224.
[19] M. Radepont, Y. Coquinot, K. Janssens, J.J. Ezrati, W. De Nolf, M. Cotte, Thermodynamic and experimental study of the degradation of the red pigment mercury sulfide, J. Anal. At. Spectrom. 30 (2015) 599–612, doi:10.1039/c4ja00372a.
[20] L. Robinet, M. Spring, S. Pagès-Camagna, D. Vantelon, N. Trcera, Investigation of the discoloration of smalt pigment in historic paintings by micro-X-ray absorption spectroscopy at the Co K-Edge, Anal. Chem. 83 (2011) 5145–5152, doi:10.1021/ac200184f.
[21] M. Vermeulen, G. Nuyts, J. Sanyova, A. Vila, D. Buti, J.P. Suuronen, et al., Visualization of As(III) and As(v) distributions in degraded paint micro-samples from Baroque- and Rococo-era paintings, J. Anal. At. Spectrom. 31 (2016) 1913–1921, doi:10.1039/c6ja00134c.
[22] L. Monico, S. Prati, G. Sciutto, E. Catelli, A. Romani, D.Q. Balbas, et al., Development of a multi-method analytical approach based on the combination of synchrotron radiation X-ray micro-analytical techniques and vibrational microspectroscopy methods to unveil the causes and mechanism of darkening of “fake-gilded” decorations in a Cimabue painting, J. Anal. At. Spectrom. 37 (2022) 114–129, doi:10.1039/D1JA00271F.
[23] H. Howard, J. Najorka, P.F. Schofield, K. Geraki, Degradation of fourteenth-century mordant gilding layers: synchrotron-based microfocus XRF, XRD, and XANES analyses of two paintings by Pietro Lorenzetti, Stud. Conserv. 69 (2024) 193–208, doi:10.1080/00393630.2023.2201094.
[24] C. Gervais, M.A. Languille, S. Reguer, M. Gillet, E.P. Vicenzi, S. Chagnot, et al., Live” Prussian blue fading by time-resolved X-ray absorption spectroscopy, Appl. Phys. Mater. Sci. Process. 111 (2013) 15–22, doi:10.1007/s00339-013-7581-y.
[25] L. Samain, F. Grandjean, G.J. Long, P. Martinetto, P. Bordet, J. Sanyova, et al., Synthesis and fading of eighteenth-century Prussian blue pigments: a combined study by spectroscopic and diffractive techniques using laboratory and synchrotron radiation sources, J. Synchrotron. Radiat. 20 (2013) 460–473, doi:10.1107/S0909049513004585.
[26] L. Monico, G. Van der Snickt, K. Janssens, W. De Nolf, C. Miliani, J. Verbeeck, et al., Degradation process of lead chromate in paintings by Vincent van Gogh

studied by means of synchrotron X-ray spectromicroscopy and related methods. 1. Artificially aged model samples, Anal. Chem. 83 (2011) 1214–1223, doi:10.1021/ac102424h.
[27] M. Ghirardello, V. Gonzalez, L. Monico, A. Nevin, D. MacLennan, C.S. Patterson, et al., Application of synchrotron radiation-based micro-analysis on cadmium yellows in Pablo Picasso's *Femme*, Microsc. Microanal. 28 (2022) 1504–1513, doi:10.1017/S1431927622000873.
[28] L. Monico, F. Rosi, R. Vivani, L. Cartechini, K. Janssens, N. Gauquelin, et al., Deeper insights into the photoluminescence properties and (photo)chemical reactivity of cadmium red ($CdS_{1-x}Se_x$) paints in renowned twentieth century paintings by state-of-the-art investigations at multiple length scales, Eur. Phys. J. Plus 137 (2022) 311, doi:10.1140/epjp/s13360-022-02447-7.
[29] S. Carboni Marri, L. Monico, F. Rosi, C. Miliani, R. Vivani, K. Janssens, et al., Discovering the dual degradation pathway of emerald green in oil paints: the effects of light and humidity, Sci. Adv. 11 (2025) 1807, doi:10.1126/sciadv.ady1807.
[30] L. Bertrand, S. Bernard, F. Marone, M. Thoury, I. Reiche, A. Gourrier, et al., Emerging approaches in synchrotron studies of materials from cultural and natural history collections, Top. Curr. Chem. 374 (2016) 7, doi:10.1007/s41061-015-0003-1.
[31] K. Janssens, G. Van der Snickt, F. Vanmeert, S. Legrand, G. Nuyts, M. Alfeld, et al., Non-invasive and non-destructive examination of artistic pigments, paints, and paintings by means of X-ray methods, Top. Curr. Chem. 374 (2016) 81, doi:10.1007/s41061-016-0079-2.
[32] M. Vermeulen, K. Janssens, J. Sanyova, V. Rahemi, C. McGlinchey, K. De Wael, Assessing the stability of arsenic sulfide pigments and influence of the binding media on their degradation by means of spectroscopic and electrochemical techniques, Microchem. J. 138 (2018) 82–91, doi:10.1016/j.microc.2018.01.004.
[33] C. de Mecquenem, M. Eveno, D. Zurbach, K. Mösl, M. Cotte, I. Reiche, Influence of the painting medium on the alteration process of smalt in oil paintings studied using combined K and Co K-edge XANES, Appl. Phys. A 130 (2024) 781, doi:10.1007/s00339-024-07943-4.
[34] E. Cato, C. Borca, T. Huthwelker, E.S.B. Ferreira, Aluminium X-ray absorption near-edge spectroscopy analysis of discoloured ultramarine blue in 20th century oil paintings, Microchem. J. 126 (2016) 18–24, doi:10.1016/j.microc.2015.11.021.
[35] A.A. Gambardella, M. Cotte, W. de Nolf, K. Schnetz, R. Erdmann, R. van Elsas, et al., Sulfur K-edge micro- and full-field XANES identify marker for preparation method of ultramarine pigment from lapis lazuli in historical paints, Sci. Adv. 6 (2020), doi:10.1126/sciadv.aay8782.
[36] F. D'Acapito, X-ray absorption spectroscopy (XAS) applied to cultural heritage, in: S. D'Amico, V. Venuti (Eds.), Handbook of Cultural Heritage Analysis, Springer Cham, 2022, pp. 45–67, doi:10.1007/978-3-030-60016-7_4.
[37] L. Monico, F. d'Acapito, M. Cotte, K. Janssens, A. Romani, G. Ricci, et al., Total electron yield (TEY) detection mode Cr K-edge XANES spectroscopy as a direct method to probe the composition of the surface of darkened chrome yellow ($PbCr_{1-x}S_xO_4$) and potassium chromate paints, Nucl. Instrum. Methods Phys. Res. B 539 (2023) 141–147, doi:10.1016/j.nimb.2023.03.040.
[38] L. Monico, A. Chieli, A. Vila, M. Cotte, W. De Nolf, A. Romani, et al., Illuminating Prussian blue fading in oil paintings: a multi-scale and multi-technique approach to mitigate synchrotron radiation X-ray induced iron photoreduction, Rend. Lincei (2026), doi:10.1007/s12210-026-01410-3.
[39] G. Seidler, D. Mortensen, A. Ditter, N. Ball, A. Remesnik, A Modern Laboratory XAFS cookbook, J. Phys. Conf. Ser. 712 (2016) 012015, doi:10.1088/1742-6596/712/1/012015.
[40] P. Zimmermann, S. Peredkov, P.M. Abdala, S. DeBeer, M. Tromp, C. Müller, et al., Modern X-ray spectroscopy: XAS and XES in the laboratory, Coord. Chem. Rev. 423 (2020) 213466, doi:10.1016/j.ccr.2020.213466.
[41] R. Fanselow, M. Sobstel, W. Błachucki, J. Szlachetko, Performance of a laboratory von Hámos type x-ray spectrometer in x-ray absorption spectroscopy study on 3d group metals, X-Ray Spectrom. 52 (2023) 247–253, doi:10.1002/xrs.3317.
[42] L. Bertrand, S. Schöeder, D. Anglos, M.B.H. Breese, K. Janssens, M. Moini, et al., Mitigation strategies for radiation damage in the analysis of ancient materials, TrAC Trends Anal. Chem. 66 (2015) 128–145, doi:10.1016/j.trac.2014.10.005.
[43] C. Gervais, M.-A. Languille, G. Moretti, S. Réguer, X-ray photochemistry of Prussian Blue cellulosic materials: evidence for a substrate-mediated redox process, Langmuir 31 (2015) 8168–8175, doi:10.1021/acs.langmuir.5b00770.
[44] C. Gervais, M. Thoury, S. Réguer, P. Gueriau, J. Mass, Radiation damages during synchrotron X-ray micro-analyses of Prussian blue and zinc white historic paintings: detection, mitigation and integration, Appl. Phys. A 121 (2015) 949–955, doi:10.1007/s00339-015-9462-z.
[45] M. Ganio, E.S. Pouyet, S.M. Webb, C.M. Schmidt Patterson, M.S. Walton, From lapis lazuli to ultramarine blue: investigating Cennino Cennini's recipe using sulfur K-edge XANES, Pure Appl. Chem. 90 (2018) 463–475, doi:10.1515/pac-2017-0502.
[46] L. Monico, M. Cotte, F. Vanmeert, L. Amidani, K. Janssens, G. Nuyts, et al., Damages induced by synchrotron radiation-based X-ray microanalysis in chrome yellow paints and related Cr-compounds: assessment, quantification, and mitigation strategies, Anal. Chem. 92 (2020) 14164–14173, doi:10.1021/acs.analchem.0c03251.
[47] D. Gianolio, How to start an XAS experiment, in: J.A. van Bokhoven, C. Lamberti (Eds.), X-ray Absorption and X-ray Emission Spectroscopy, Theory and Applications, John Wiley & Sons, Ltd, 2016, pp. 99–124.
[48] N.S. Genz, A. Kallio, F. Meirer, S. Huotari, B.M. Weckhuysen, Operando laboratory-based X-ray absorption spectroscopy: guidelines for newcomers in the field, Chem.–Methods 4 (2024), doi:10.1002/cmtd.202300027.
[49] K. Klementiev, R. Chernikov, XAFSmass: a program for calculating the optimal mass of XAFS samples, J. Phys. Conf. Ser. 712 (2016) 012008, doi:10.1088/1742-6596/712/1/012008.
[50] E.A. Stern, K. Kim, Thickness effect on the extended-x-ray-absorption-fine-structure amplitude, Phys. Rev. B 23 (1981) 3781–3787, doi:10.1103/PhysRevB.23.3781.
[51] C. Schlesiger, S. Praetz, R. Gnewkow, W. Malzer, B. Kanngießer, Recent progress in the performance of HAPG based laboratory EXAFS and XANES spectrometers, J. Anal. At. Spectrom. 35 (2020) 2298–2304, doi:10.1039/D0JA00208A.
[52] B. Ravel, M. Newville, ATHENA, ARTEMIS, HEPHAESTUS: data analysis for X-ray absorption spectroscopy using IFEFFIT, J. Synchrotron. Radiat. 12 (2005) 537–541, doi:10.1107/S0909049505012719.
[53] B. Ravel, M. Newville, ATHENA and ARTEMIS, in: C.T. Chantler, F. Boscherini, B. Bunker (Eds.), X-ray Absorption Spectroscopy and Related Techniques, X-ray Absorption Spectroscopy and Related Techniques, I, 2020, pp. 723–727, doi:10.1107/S1574870720003353.
[54] A. Gaur, B.D. Shrivastava, S.K. Joshi, Copper K-edge XANES of Cu(I) and Cu(II) oxide mixtures, J. Phys. Conf. Ser. 190 (2009) 012084, doi:10.1088/1742-6596/190/1/012084.
[55] O. Bunău, Y. Joly, Self-consistent aspects of x-ray absorption calculations, J. Phys.: Condens. Matter 21 (2009) 345501, doi:10.1088/0953-8984/21/34/345501.
[56] S. Rojsatien, A. Mannodi-Kanakkithodi, T. Walker, T. Nietzold, E. Colegrove, B. Lai, et al., Quantitative analysis of Cu XANES spectra using linear combination fitting of binary mixtures simulated by FEFF9, Radiat. Phys. Chem. 202 (2023) 110548, doi:10.1016/j.radphyschem.2022.110548.
[57] S. Švarcová, D. Hradil, J. Hradilová, Z. Čermáková, Pigments—copper-based greens and blues, Archaeol. Anthr. Sci. 13 (2021), doi:10.1007/s12520-021-01406-0.
[58] S. Praetz, C. Schlesiger, D.A. Motz, S. Klimke, M. Jahns, C. Gottschalk, et al., Can laboratory-based XAFS compete with XRD and Mössbauer spectroscopy as a tool for quantitative species analysis? Critical evaluation using the example of a natural iron ore, PLoS One 20 (2025) e0323678, doi:10.1371/journal.pone.0323678.
[59] J. Zhu, Z. Zeng, W.-X. Li, K-Edge XANES investigation of Fe-based oxides by density functional theory calculations, J. Phys. Chem. C 125 (2021) 26229–26239, doi:10.1021/acs.jpcc.1c08461.
[60] L.X. Chen, T. Liu, M.C. Thurnauer, R. Csencsits, T. Rajh, Fe_2O_3 nanoparticle structures investigated by X-ray absorption near-edge structure, surface modifications, and model calculations, J. Phys. Chem. B 106 (2002) 8539–8546, doi:10.1021/jp025544x.
[61] M. Batiashvili, M. Gallinaro, F.B. Restelli, L. Medeghini, C. Young, M. Botticelli, Colour of the past in South Caucasus: the first archaeometric investigation on rock art and pigment residues from Georgia, Quat. Int. 658 (2023) 1–13, doi:10.1016/j.quaint.2023.03.019.
[62] J.-M. Triat, Les Ocres, CNRS éd, Paris, 2010.
[63] Eastaugh N., Walsh V., Siddall R., Chaplin T. Pigment compendium: a dictionary and optical microscopy of historical pigments. vol. 1. 2008.
[64] M. Jercher, A. Pring, P.G. Jones, M.D. Raven, Rietveld X-ray diffraction and X-ray fluorescence analysis of Australian aboriginal ochres, Archaeometry 40 (1998) 383–401, doi:10.1111/j.1475-4754.1998.tb00845.x.
[65] M. Elias, C. Chartier, G. Prévot, H. Garay, C. Vignaud, The colour of ochres explained by their composition, Mater. Sci. Eng. B Solid. State Mater. Adv. Technol. 127 (2006) 70–80, doi:10.1016/j.mseb.2005.09.061.
[66] M. Botticelli, F. Altamura, E. Catelli, L. Pronti, L. Medeghini, M. Mussi, et al., Colorimetric characterization of ochres in a palaeolithic flint pebble from Maschio dell'Artemisio, Latium, Italy, J. Archaeol. Sci. Rep. 43 (2022) 103420, doi:10.1016/j.jasrep.2022.103420.
[67] L.P. Pierre, B. Marc, J. Amélie, R. Jean-Pascal, D. Manoj, M. Guillaume, et al., Local environment of arsenic in sulfide minerals: insights from high-resolution X-ray spectroscopies, and first-principles calculations at the As K-edge, J. Anal. At. Spectrom. 33 (2018) 2070–2082, doi:10.1039/C8JA00272J.
[68] K. Keune, J. Mass, F. Meirer, C. Pottasch, A. van Loon, A. Hull, et al., Tracking the transformation and transport of arsenic sulfide pigments in paints: synchrotron-based X-ray micro-analyses, J. Anal. At. Spectrom. 30 (2015) 813–827, doi:10.1039/C4JA00424H.
[69] F.T.H. Broers, K. Janssens, J. Nelson Weker, S.M. Webb, A. Mehta, F. Meirer, et al., Two pathways for the degradation of orpiment pigment (As_2S_3) found in paintings, J. Am. Chem. Soc. 145 (2023) 8847–8859, doi:10.1021/jacs.2c12271.
[70] F.P. Romano, E. Puglia, C. Caliri, D.P. Pavone, M. Alessandrelli, A. Busacca, et al., Layout of ancient Greek papyri through lead-drawn ruling lines revealed by Macro X-ray fluorescence imaging, Sci. Rep. 13 (2023) 1–11, doi:10.1038/s41598-023-33242-8.
[71] M. Botticelli, R. Andolina, M. Cardinali, A. Cerasuolo, S. Gammino, C. Miliani, et al., Raphael seen through MA-XRF: understanding the master and his atelier by studying the Capodimonte collection, J. Cult. Herit. 77 (2026) 156–167, doi:10.1016/j.culher.2025.11.004.
[72] C. Santoro, K. Zarkout, A.-S. Le Hô, F. Mirambet, D. Gourier, L. Binet, et al., New highlights on degradation process of verdigris from easel paintings, Appl. Phys. A 114 (2014) 637–645, doi:10.1007/s00339-014-8253-2.
[73] M. Vermeulen, J. Sanyova, K. Janssens, G. Nuyts, S. De Meyer, K. De Wael, The darkening of copper- or lead-based pigments explained by a structural modifi-

cation of natural orpiment: a spectroscopic and electrochemical study, J. Anal. At. Spectrom. 32 (2017) 1331–1341, doi:10.1039/C7JA00047B.
[74] L. Bertrand, S. Schöder, I. Joosten, S.M. Webb, M. Thoury, T. Calligaro, et al., Practical advances towards safer analysis of heritage samples and objects, TrAC Trends Anal. Chem. 164 (2023) 117078, doi:10.1016/j.trac.2023.117078.
[75] F. Farges, M. Cotte, X-ray absorption spectroscopy and cultural heritage: highlights and perspectives, in: J.A. van Bokhoven, C. Lamberti (Eds.), X-Ray Absorption and X-Ray Emission Spectroscopy, John Wiley & Sons, Ltd, 2016, pp. 609–636, doi:10.1002/9781118844243.ch21.